2017-12

Sea-ice dynamics in an Arctic coastal polynya during the past 6500years

Knies, J

10.1007/s41063-016-0027-y
arktos
Springer Science and Business Media LLC

Arktos _####################_
DOI 10.1007/s41063-016-0027-y

ORIGINAL ARTICLE

Sea-ice dynamics in an Arctic coastal polynya during the past 6500 years

Jochen Knies[1,2,3] · Irene Pathirana[1,3] · Patricia Cabedo-Sanz[4] · Ana Banica[1] · Karl Fabian[1,2,3] · Tine L. Rasmussen[2,3] · Matthias Forwick[3] · Simon T. Belt[4]

Received: 7 September 2016 / Accepted: 2 December 2016

Abstract The production of high-salinity brines during sea-ice freezing in circum-arctic coastal polynyas is thought to be part of northern deep water formation as it supplies additional dense waters to the Atlantic meridional overturning circulation system. To better predict the effect of possible future summer ice-free conditions in the Arctic Ocean on global climate, it is important to improve our understanding of how climate change has affected sea-ice and brine formation, and thus finally dense water formation during the past. Here, we show temporal coherence between sea-ice conditions in a key Arctic polynya (Storfjorden, Svalbard) and patterns of deep water convection in the neighbouring Nordic Seas over the last 6500 years. A period of frequent sea-ice melting and freezing between 6.5 and 2.8 ka BP coincided with enhanced deep water renewal, while near-permanent sea-ice cover and low brine rejection after 2.8 ka BP likely reduced the overflow of high-salinity shelf waters, concomitant with a gradual slow down of deep water convection in the Nordic Seas, which occurred along with a regional expansion in sea-ice and surface water freshening. The Storfjorden polynya sea-ice factory restarted at ~0.5 ka BP, coincident with renewed deep water penetration to the Arctic and climate amelioration over Svalbard. The identified synergy between Arctic polynya sea-ice conditions and deep water convection during the present interglacial is an indication of the potential consequences for ocean ventilation during states with permanent sea-ice cover or future Arctic ice-free conditions.

Keywords Arctic · Storfjorden · Polynya · Holocene · Sea ice

Introduction

The sinking of dense waters on Arctic and Antarctic shelves through recurrent cooling and rejection of salt during sea-ice growth is a key contributor to global ocean circulation [24] with 10% of contemporary deep waters formed in the Arctic Ocean and the Barents Sea derived from these brine-enriched shelf waters [32]. High sea-ice production in Arctic coastal polynyas facilitates dense water production and ocean stratification, thus inhibiting the upward mixing of warm Atlantic water and sea-ice melt [1]. Coastal polynyas are persistent and recurrent areas of open water that occur within locations of otherwise consolidated and thicker ice cover. Amongst these, the Storfjorden coastal polynya in southern Spitsbergen (Fig. 1) is known to be an important sea-ice factory [19] and a significant source of brine rejection [32]. Dense brine-enriched waters from Storfjorden cascade downslope before flowing north [41], where they descend to depths of more than 2000 m [23] and account for up to 15% of the total dense water generated in the entire Arctic [13, 43]. However, this has likely changed in the past either as a contributor to, or because of climate change at high latitudes. Indeed, millennial-scale reconstruction of past brine

✉ Jochen Knies
jochen.knies@ngu.no

[1] Geological Survey of Norway, 7491 Trondheim, Norway

[2] CAGE-Centre for Arctic Gas Hydrate, Environment and Climate, Tromsø, Norway

[3] Department of Geology, UiT The Arctic University of Norway, 9037 Tromsø, Norway

[4] Biogeochemistry Research Centre, School of Geography, Earth and Environmental Sciences, University of Plymouth, Plymouth PL4 8AA, UK

Journal : Large 41063 | Dispatch : 16-12-2016 | Pages : 15
Article No. : 27 | ☐ LE | ☐ TYPESET
MS Code : ARCT-D-16-00010 | ☑ CP | ☑ DISK

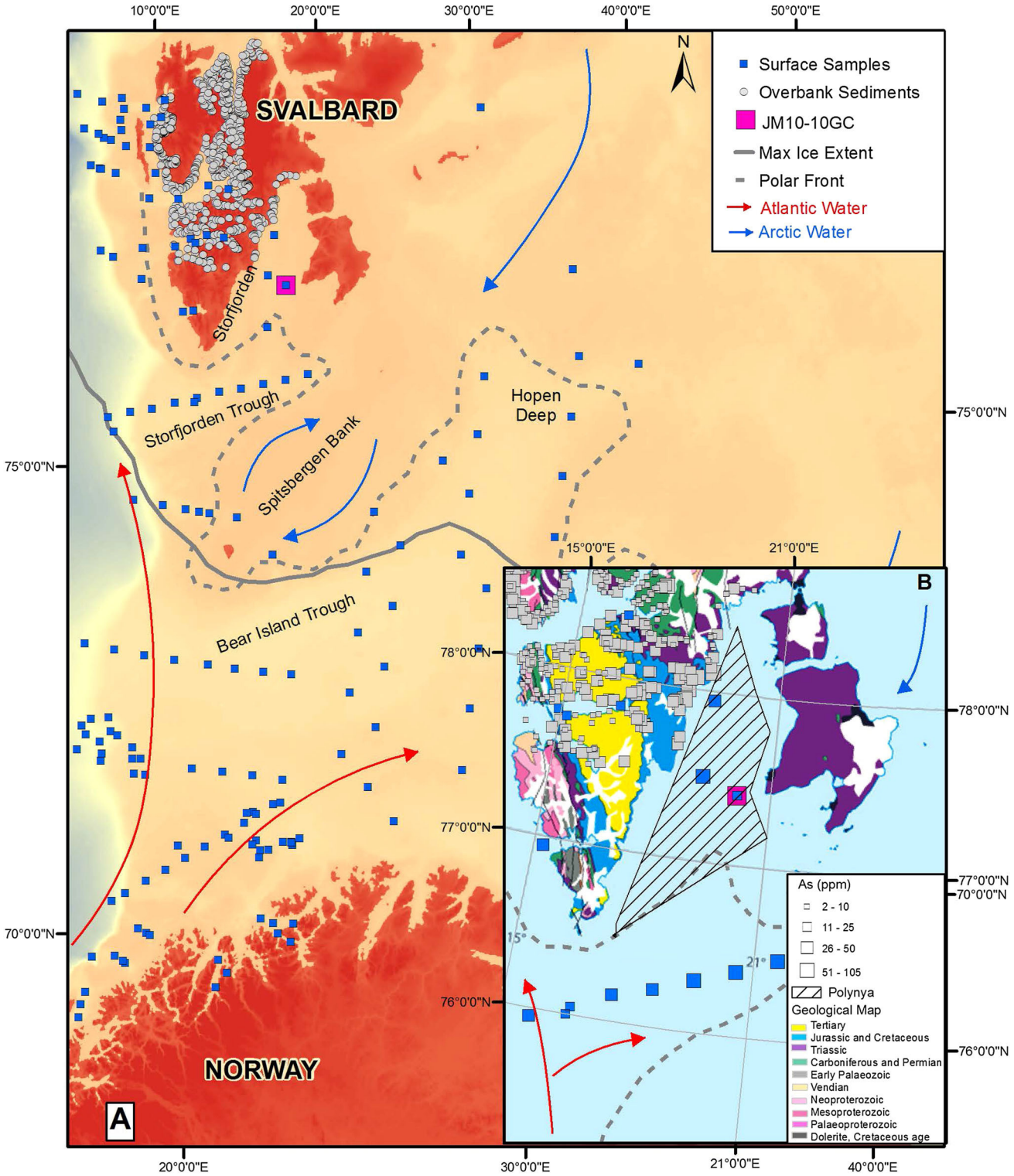

Fig. 1 Study area and investigated marine sediment surface, floodplain and core samples. Major oceanographic features and the maximum sea ice extent are indicated. *Inset* shows outline of Storfjorden Polynya (*grey shaded*) superimposed on the geology of Svalbard. Arsenic concentrations (ppm) in both floodplain sediments onshore and marine surface sediments are shown

formation in the Storfjorden polynya based on the sedimentary distribution of calcareous and agglutinated benthic foraminifera has revealed a systematic pattern of high (low) intensities during cold (warm) climate periods over the last 15,000 years [34, 35]. In contrast, large annual variability in brine formation has also been observed

Journal : Large 41063 Dispatch : 16-12-2016 Pages : 15
Article No. : 27 LE TYPESET
MS Code : ARCT-D-16-00010 CP DISK

during the most recent warm periods during the last century. Thus, reduced brine formation, and hence, strongly reduced export of dense water to the Arctic Ocean occurred during periods with exceptionally warm Atlantic water advection and reduced sea-ice coverage in the Barents Sea, while intense brine formation was re-established during periods of recurrent cooling [58]. Accordingly, since the process of brine rejection is largely dependent on the seasonal formation of sea-ice, past reconstruction of sea-ice coverage coupled with environmental inferences from benthic foraminifera assemblages in the Storfjorden polynya [34, 35] provides a more direct indication of past brine formation, and thus potentially, a new measure for evaluating the significance of Arctic coastal polynyas with respect to dense water formation on a glacial-interglacial timescale. This approach provides an alternative to the still disputed use of benthic foraminiferal stable isotope records as a measure of the influence of brine-enriched shelf waters on deep water production [15, 28, 33]. In this study, we combine down-core records of organic geochemical biomarkers of sea-ice variability (IP_{25}) [8] and open water phytoplankton (brassicasterol) with source-specific, sea-ice derived terrigenous sediments, supplemented by published agglutinated foraminifera (% of total benthic foraminifera) [34, 35]. We hereby present evidence that changes in sea-ice coverage and inferred brine formation in the Storfjorden polynya over the past 6500 years coincide with past variability in deep water renewal in the Nordic Seas. As such, we highlight the importance of Arctic coastal polynyas as one significant driver of deep water renewal processes during the present interglacial.

Regional setting

Storfjorden, in southeastern Spitsbergen, is a ca. 200-km-long inlet, separated from the open ocean by a shallow sill (~120 m). Surface waters are seasonally stratified, with sea-ice and brine formation taking place each winter in the inner fjord [41]. Strong northeasterly winds blow sea-ice away from the eastern shelf, producing a large latent heat polynya, where high sea-ice production and continuous freezing generates cold (<−1.9 °C) and salty (34.8 to >35.8 psu) water [19, 43], which sinks and fills the central basin, finally overflowing the sill. Depending on its salinity (34.3–35.3 psu) [43], the brine may continue downslope reaching 2000 m into the deep-intermediate water of the Greenland Sea [23, 32]. Surface currents in Storfjorden are controlled by southwestward flowing, ice-covered polar waters from the Arctic Ocean. The East Spitsbergen Current (ESC) balances the bottom currents that transport the dense water out of Storfjorden towards the deep ocean. Sediments deposited in Storfjorden are enriched in organic carbon (up to 2.4 wt%) and largely dominated by terrigenous derived organic matter [56]. Terrigenous sediments are largely supplied by local (fast) ice entrainment processes and episodic freezing/melting processes in the polynya. Alternatively, terrigenous sediments transported by polar surface waters (ESC) to Storfjorden are released during frequent melting episodes and are deposited in Storfjorden [56].

Materials and methods

We studied inorganic elements and organic biomarkers in sediment surface samples (0–1 cm) taken with multicorer equipment from the western Barents Sea (Fig. 1; Table 1) and a gravity core JM10-10GC (77.41°N, 20.10°E, 123 m water depth, hereafter referred to as JM10), taken within the Storfjorden polynya where brines form today (Fig. 1). The surface samples were sliced onboard, frozen, and subsequently freeze-dried prior to analysis.

Inorganic geochemistry

All surface samples were analysed for major and trace elements using a Philips PW 1480 WD XRF instrument equipped with an Rh X-ray tube. For XRF major elements about 2 g of finely ground sample was preheated over a gas burner to remove any organic material before pre-ignition at 1000 ± 50 °C for at least 1 h. 4.200 ± 0.005 g $Li_2B_4O_7$ (Claisse, Quebec, Canada) is mixed with 0.600 ± 0.005 g pre-ignited sample and fused to glass beads in Pt—5% Au-crucible. The method for determination of trace element with XRF is based on pressed pellets. 1.2 ± 0.005 g Hoechst wax was mixed with 5.4 ± 0.005 g dried and fine-ground sample material in a Spex Mixer/Mill for at least 1 min. The mixture was pressed to a pellet in a Herzog pelletizing press, with an applied force around 20 kN for 20 s. Methods accuracy for arsenic (As) and aluminium (Al) was tested with several certified reference materials (CRM), as shown in Tables 2 and 3. Relative percent difference between the duplicate samples was within ±10%. Al-normalisation was applied for As data in core JM10 to avoid dilution due to variable sedimentation rates (19–104 cm/ka) in the record [34]. A correlation coefficient $R^2 = 0.88$ between As/Al ratio and As concentrations (ppm) in core JM10 indicate no dilution effects on the As concentrations in the sediments.

Concentration of leachable elements in the same sample set was measured by ICP-AES with the instrument PerkinElmer 4300 DV. Nitric acid extraction was used to estimate the amounts of As and Al present in the nonsilicate fraction of the sediment in all surface sediments and core JM10. 1.000 ± 0.001 g of freeze-dried sediment was

Journal : Large 41063 Dispatch : 16-12-2016 Pages : 15
Article No. : 27 LE TYPESET
MS Code : ARCT-D-16-00010 CP DISK

Table 1 Inorganic geochemical data from Barents Sea surface sediments

Station ID	Latitude	Longitude	Water depth (m)	As (ppm)		Al (ppm)		Mn (ppm)		Fe (ppm)	
				ICP-AES	XRF	ICP-AES	XRF	ICP-AES	XRF	ICP-AES	XRF
623	71.05	21.65	166	13	6	20,200	62,768	933	929	31,300	33,573
627	72.32	24.06	264	4	6	13,100	54353	435	620	17,500	24,690
629	73.01	24.25	404	5	14	19,700	66949	704	1084	25,600	38050
631	73.67	24.47	451	9	10	22,400	68,907	483	620	32300	39,449
633	74.34	24.69	373	22	26	13700	57,264	471	465	29,000	36,931
635	75.00	24.94	182	12	16	17,200	60,016	204	232	25,100	29,866
639	75.57	27.90	263	19	23	22,700	71,236	277	310	33,800	40,148
643	76.49	29.91	291	7	9	22,600	72,294	190	232	29,400	36,581
645	75.86	29.46	296	25	23	18,200	67,372	163	232	33,900	39,309
647	75.20	29.01	343	14	28	19,600	72,241	277	465	29,000	44,345
649	74.54	28.58	394	22	27	20,700	64,885	543	697	32,700	39,239
651	74.64	26.08	317	18	29	20,100	64,461	745	929	32,500	38,959
653	73.97	25.81	441	9	11	22,700	73,512	251	310	32,000	40,008
655	73.31	25.54	412	10	15	19,800	67,319	539	697	30,300	38,190
657	72.64	25.27	268	6	10	11,000	54,035	261	387	16,500	24,341
659	71.98	25.06	256	2	5	9730	49,325	245	387	13,400	20,144
661	71.37	22.76	408	3	5	19,400	64,779	421	620	25,300	35,322
663	71.61	25.99	291	1	3	6560	42,392	187	387	9480	15,808
665	72.17	28.41	289	3	6	12,600	56,629	193	310	16,800	24,830
667	72.84	28.76	305	11	13	13,300	54,618	336	387	23,100	27,278
669	73.50	29.15	414	8	11	19,600	67,478	375	465	28,700	36,022
671	74.15	29.55	366	13	21	22,600	73,194	330	387	35,100	43,925
673	74.67	32.49	165	20	19	11,300	50,595	198	232	23,900	27,488
675	75.33	33.07	209	18	58	15,700	52,395	199	232	31,700	28,118
677	75.97	33.73	276	14	21	22,900	78,433	193	232	31,400	38,959
679	76.62	34.45	193	105	157	20,100	65,097	523	620	58,400	75,261
681	76.43	37.17	249	13	15	11,000	59,645	102	155	18,100	22,802
690	71.02	30.96	283	8	8	23,200	64,938	354	465	27,200	35,462
692	70.62	31.72	252	2	5	7280	45,885	190	232	10,900	17,556
St.l.	72.00	22.00	367	6	7	19,300	61,762	604	852	24,700	32,454
St.2.	72.02	20.92	371	7	8	21,900	63,932	1040	1317	28,300	35,532
St.3.	72.03	19.85	324	9	11	18800	50,966	725	929	23,000	29,377
St.4.	72.02	18.77	315	9	12	17,200	47,208	770	1084	20,700	27,348
St.5.	72.03	17.70	296	8	7	13,200	45,250	668	929	17,500	23,991
St.6.	72.02	16.62	362	8	3	9300	41,757	366	542	14,500	20,844
St.7.	72.02	15.52	767	10	12	8390	43,345	369	620	15,900	24,551
St.8.	72.01	14.73	1260	7	fi	18,000	65,573	336	465	25,700	33,084
St.9.	72.01	14.62	1317	7	6	13,500	51,707	873	1239	17000	25,740
St.11.	73.17	12.94	1499	8	6	14,600	46,467	854	1162	18,300	24,760
St.12.	73.17	14.09	1030	5	3	10,300	44,668	555	852	13,600	22,312
St.13.	73.17	15.23	485	8	11	8800	48,426	386	542	12,900	18,815
St.14.	73.17	16.38	475	8	11	12,500	54,088	434	542	18,000	24,411
St.15.	73.17	17.54	460	9	12	14,300	54,935	459	542	21,300	26,229
St.16.	73.17	18.82	423	16	18	12,700	52,977	421	542	21,900	26,929
St.17.	73.17	19.86	441	7	8	14,400	55,941	350	465	20,500	25,949
St.18.	73.17	20.95	463	12	15	17,900	62,768	642	774	27,000	33,713
St.19.	73.17	22.01	444	15	21	18,300	62,662	938	1084	27,900	34,832

Journal : Large 41063 Dispatch : 16-12-2016 Pages : 15
Article No. : 27 LE TYPESET
MS Code : ARCT-D-16-00010 CP DISK

Table 1 continued

Station ID	Latitude	Longitude	Water depth (m)	As (ppm)		Al (ppm)		Mn (ppm)		Fe (ppm)	
				ICP-AES	XRF	ICP-AES	XRF	ICP-AES	XRF	ICP-AES	XRF
St.20.	74.82	18.02	296	18	25	11,100	41,969	326	387	20,900	25,810
St. 21.	74.82	17.00	280	7	7	8120	35,353	212	310	14,700	18,465
St. 22.	74.82	16.03	356	8	7	10,100	42,763	275	387	16,900	20,354
St.23.	74.82	14.79	1507	9	10	19,200	52,448	1120	1471	23,600	30,636
St.24.	75.64	12.92	1500	10	14	18,900	51,971	1260	1626	24,000	31,055
St.25.	75.75	13.84	807	18	20	13,100	54,512	518	697	24,300	30,426
St.26.	75.83	14.77	370	18	25	19,200	66,949	800	929	31,600	36,511
St.27.	75.95	15.72	369	45	59	21,500	71,236	3650	4337	42,300	49,031
St.28.	76.05	16.67	328	21	25	17,200	63,509	942	1084	31,300	36,441
St.29.	76.16	17.62	309	45	57	20,500	67,108	1340	1549	40,200	44,625
St.30.	76.22	18.58	257	31	33	20,200	67,849	577	697	36,800	41,058
St.31.	76.31	19.57	258	53	66	19,400	70,019	2160	2556	42,100	49,801
St.32.	76.38	20.58	228	54	68	19,600	69,278	787	929	44,000	48,891
St.33.	76.47	21.60	262	91	117	20,200	71,447	1050	1239	46,900	53,927
St.34.	71.75	22.00	356	4	3	18,800	61,127	504	697	24,200	32,804
St.35.	71.62	21.07	319	5	6	13,900	51,813	490	697	17,800	24,970
St.36.	71.60	20.86	320	7	7	14,400	48,902	646	852	18,800	25,390
St.37.	71.60	21.19	335	5	6	14,300	53,347	464	620	18,600	25,460
St.38.	71.49	20.82	310	6	3	15,800	46,520	651	929	19,700	25,880
St.39.	71.34	20.19	234	5	5	13,800	39,958	695	1007	16,900	23,431
St.40.	71.18	19.56	225	6	3	12,700	39,111	718	1007	15,700	21,963
St.41.	71.03	18.95	199	1	3	6390	35,830	266	465	9060	15,598
St.42.	70.87	18.34	173	3	3	5860	23,657	219	387	8090	13,499
St.43.	70.72	17.75	273	7	5	11,300	41,651	606	929	14,700	22,382
St.44.	70.55	17.14	706	3	7	7290	39,746	274	620	9690	19,794
St.45.	70.44	16.75	1500	6	7	9350	53,136	517	929	14,000	26,859

Table 2 Methods accuracy for measuring As by XRF

Parameter	UB-N	MESS-1	JLK-1
Sample type	Serpentine	Marine sediment	Lake sediment
Average, three replicates, mg/kg	10.94	7.9	26.91
Standard deviation, three replicates, mg/kg	2.5	0.77	3.43
%RSD	23.20%	9.80%	12.80%
Certified value, mg/kg	10[a]	10.6	27.7
Uncertainty, mg/kg	4.22	1.2	
References GeoReM	GeoReM 149	GeoReM 5021	
Bias, mg/kg	0.94	−2.7	−0.79
Relative bias	9.40%	−25.50%	−2.90%

[a] Compiled value

digested with 20 ml 7 M HNO_3 for 30 min at 120 ± 4 °C in autoclave (CertoClav Sterilizer, CV-EL 18LGS), following the procedure described in the Norwegian Standard NS 4770 from 1994. After cooling, the sample was filtered through Whatman grade 597 and further diluted. The analysed solution contains 10 ppm Rh as internal standard and about 10% HNO_3 (v/v). Method quantification limits, respectively, 20 mg/kg Al and 2 mg/kg As, is based on ten times the standard deviation for ten replicates of method blanks. Relative percent difference between the duplicate samples was within ±10%. Certified reference material Mess-3 (marine sediment for trace elements and other

Journal : Large 41063 Dispatch : 16-12-2016 Pages : 15
Article No. : 27 LE TYPESET
MS Code : ARCT-D-16-00010 CP DISK

Table 3 Methods accuracy for measuring Al by XRF

Parameter	PACS-1	MESS-1	JLK-1
Sample type	Marine sediment	Marine sediment	Lake sediment
Measured, %	12.06	12.05	16.77
Certified value, %	12.23	11.03[a]	16.73
Uncertainty, %	0.22	0.38	0.184
References GeoReM (Jochum et al. 2005)	GeoReM 5021	GeoReM 5021	GeoReM 659
Bias, mg/kg	−0.17	1.03	−0.04
Relative bias	−1.37%	9.26%	−0.23%

[a] Compiled value

constituents, NRC-CNRC Canada) was routinely analysed to test methods analytical performance. The correlation coefficients between XRF and ICP-AES based arsenic and aluminium concentrations of 73 surface samples is $r^2 = 0.95$ and 0.75, respectively. Arsenic concentrations in the remaining text are based on the ICP-AES extraction method to allow comparison with published As concentration in floodplain and overbank deposits from Spitsbergen [31] (Fig. 1).

Biomarkers

The biomarkers IP_{25} [8] and brassicasterol were quantified following addition of internal standards (9-octylheptadec-8-ene, 10 µL; 10 µg mL^{-1}; 5α-androstan-3β-ol, 10 µL; 10 µg mL^{-1}, respectively), extraction (DCM/Methanol; 3 × 3 mL, 2:1 v/v) and purification of extracts using silica column chromatography (IP_{25}: hexane, 6 mL; brassicasterol: 20:80 methylacetate/hexane, 6 mL). Further purification of the IP_{25} containing fraction was achieved by Ag-ion chromatography (Supelco discovery Ag-Ion; 0.1 g) with saturated hydrocarbons (hexane; 1 mL) and unsaturated hydrocarbons (including IP_{25}: acetone; 2 mL) eluted as two single fractions. All partially purified fractions were analysed using gas chromatography–mass spectrometry (GC–MS) according to established methods [5]. Brassicasterol was derivatized (BSTFA; 50 µL, 70 °C, 1 h) prior to analysis by GC–MS.

Chronology

The chronology of the upper 325 cm of JM10 is based on 7 AMS ^{14}C radiocarbon dates obtained on bivalves and monospecific samples of the benthic foraminiferal species *N. labradorica* (Table 4) (see details in [35]. All AMS ^{14}C dates were calibrated to calendar ages by applying the Calib7.02 programs [45] and the Marine13 calibration curve [38]. The applied age model is consistent with the published model of Rasmussen and Thomsen [35]. The sedimentation rates vary between 19 and 104 cm/ka, with highest values (104 cm/ka) in the upper part of the sediment cores (~1.0–0.5 ka BP), and lowest values (19 cm/ka) between ~2.8 and ~1.0 ka BP. Moreover, sedimentation rates in the lowermost part of the record (2.8 to ~6.5 ka BP) vary between 49 and 76 cm/ka. The quality of the dated material was checked by measuring bivalves and *N. labradorica* in two different samples within the same depth interval (324–326 cm). The dates are identical within error (Table 4), excluding the possibility of re-deposition of the bivalves in this environmental setting. However, we caution the reader that the observed changes in sedimentation rates between 2.8 and 1.0 ka BP are based on dating results from bivalves only, due to the lack of sufficient planktic or benthic foraminifera in this interval.

Results and discussion

Proxies for sea-ice dynamics

To interpret our down-core record, we first provide the background to our combined proxy data by presenting measurements obtained from surface sediments that reflect the modern physico-geography of the region. Arsenic (As) concentration in near-shore unpolluted marine sediments is normally between 5 and 10 ppm [52]. Sedimentary arsenic is principally associated with sesquioxide material (mostly hydrous iron oxides) as shown by a positive correlation between As and Fe ($r^2 = 0.65$). Arsenic concentration in our Barents Sea surface sediments varies between 2 and 105 ppm, with a clear geographical boundary along the Marginal Ice Zone (MIZ) (Fig. 2). South of the MIZ, the mean As concentration (7 ppm) resembles values in uncontaminated soils from northern Scandinavia [37], while for sites north of the MIZ, a mean concentration of 27 ppm is significantly higher than the global average for coastal marine sediments (5–10 ppm; [52]). The enrichment in the northern sediments is, however, probably not related to diagenetic redox-cycling processes seen in other shelf environments [46] since As anomalies are not correlated with other redox-sensitive elements such as Mn ($r^2 < 0.2$). Instead, it is more likely that natural sources of

Journal : Large 41063 Dispatch : 16-12-2016 Pages : 15
Article No. : 27 LE TYPESET
MS Code : ARCT-D-16-00010 CP DISK

Table 4 AMS^{14}C dates and calibrated dates for core JM10-10GC as published by Rasmussen and Thomsen [34, 35]

Core ID	Depth (cm)	14C Age	Calendar age	Lab. code	Species
JM10-10GC	44.5	832 ± 21	473 ± 20	UB-17204	*Nucula* sp.
JM10-10GC	102.5	1491 ± 22	1029 ± 43	UB-17205	*Nuculana* sp.
JM10-10GC	136.5	3008 ± 27	2770 ± 32	UB-17206	*Astarte* sp.
JM10-10GC	210.5	4182 ± 41	4278 ± 73	UB-18845	*N. labradorica*
JM10-10GC	250.5	4573 ± 28	4805 ± 34	UB-18946	*N. labradorica*
JM10-10GC	324–326	6065 ± 31	6482 ± 49	UB-17207	*Bivalve*
JM10-10GC	325	5990 ± 43	6398 ± 57	UB-21198	*N. labradorica*

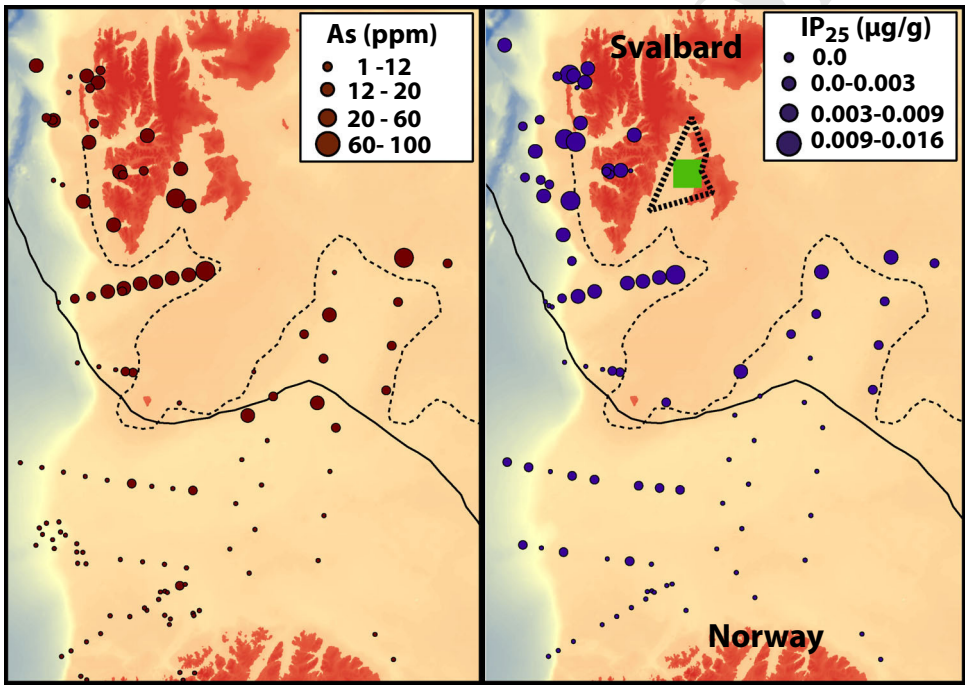

Fig. 2 Proxy data for modern sea-ice variability in the Barents Sea. *Left* Arsenic concentration (As in ppm) in Barents Sea surface samples. *Right* Sea-ice biomarker IP_{25} concentration in Barents Sea surface samples [30]. Storfjorden Polynya (*stippled polygon*), studied core position JM10 (*green square*), maximum of marginal ice zone (MIZ) (*black line*) and the Barents Sea polar front (*stippled line*) are indicated

As-rich deposits and dissolved As in the water column are the causes of the sedimentary enhancements. As-rich sediments are most likely transported by sea-ice and released along the MIZ [21], while dissolved As can be taken up by phytoplankton blooms in the MIZ, and thus incorporated into the sedimentary cycle [10]. Indeed, local As anomalies are reported from Paleogene sequences, SW Spitsbergen (Fig. 1) [31] and As concentrations as high as 225 ppm have been recorded in coal seams interbedded with marine and lacustrine siltstones and shales [22]. Arsenic anomalies (>50 ppm) also occur in nearby floodplain sediments sourced from Carboniferous-Cretaceous organic-rich deposits along the coastline adjacent to Storfjorden (Fig. 1) [31]. Coastal freezing processes along the shoreline or within coastal polynyas [16] allow entrainment of As-enriched sediments in sea-ice with subsequent release during melt within the MIZ. Other As anomalies in sediments are reported from the Laptev Sea and Kara Sea shelves [21, 26, 27], where incorporation of As-enriched particles in newly formed sea-ice and transportation within the Transpolar Drift and East Spitsbergen Current may have caused the As anomalies identified below the MIZ in the northwestern Barents Sea (Fig. 2). Hence, we use the As anomalies in the sedimentary record as evidence for newly formed sea-ice that allowed incorporation of terrigenous (As-rich) particles in coastal areas, and subsequent sea-ice melting and release of As-rich ice-rafted sediments within the MIZ. To complement the As data, we also measured the distribution of the organic geochemical sea-ice proxy IP_{25} in the same surface sediments. IP_{25} is a highly specific lipid biosynthesized by certain diatoms residing in the underside of seasonal Arctic sea-ice [11] and whose presence and abundance in sediments is strongly associated with overlying sea-ice cover [6, 8], including the Barents Sea [7, 30]. In general, higher or increasing sedimentary abundances of IP_{25} are positively associated with seasonal sea-ice occurrence (or change) as shown through various surface and down-core records from across the Arctic [6]. However, lower IP_{25} abundances have been found in sediments from regions of much higher or near-permanent sea-ice cover

Journal : Large 41063 Dispatch : 16-12-2016 Pages : 15
Article No. : 27 LE TYPESET
MS Code : ARCT-D-16-00010 CP DISK

including East Greenland [3] and the High Arctic (>80°N) [50, 57]. In such settings, the abundances of phytoplankton biomarkers, including brassicasterol, are also low; both observations being consistent with light-inhibited and therefore low biological productivity.

Sea-ice dynamics in an Arctic coastal polynya

The accumulation of IP_{25} in the MIZ sediments [30] closely resembles the spatial distribution of As (Fig. 2) consistent with recurrent freezing and melting of sea-ice in the region. Furthermore, the release of sea-ice debris is known to stimulate phytoplankton blooms during spring, resulting in high export production rates during peak-bloom stages within the MIZ [36]. Through particle scavenging, this provides an additional mechanism that leads to enhanced sedimentary As. Down-core analyses of these sea-ice (IP_{25}, As) and phytoplankton (brassicasterol) proxies (Fig. 3), therefore, provide a temporal measure of variable sea-ice coverage in the Storfjorden polynya, and by inference, changes in high-salinity brine rejection due to variable polynyal activity resulting from freezing/melting processes. The results are discussed for three different time intervals (6.5–2.8, 2.8–0.5, <0.5 ka BP), with the boundary at 2.8 ka based on the gradual decline of the IP_{25} concentration between 3.0 and 2.5 ka and the abrupt increase in percentages of agglutinated forams at this time (Fig. 4). Notched box-whisker plots for the distributions of As/Al, IP_{25}, and brassicasterol in these time intervals (Fig. 3) confirm that, for all parameters, the median in the interval 2.8–0.5 ka is largely different from the median in the time intervals 6.5–2.8 and 0.5–0 ka on 5% level. However, on a 5% level, notched regions of As/Al distribution in intervals 2.8–0.5 and 0.5–0 ka do overlap (Fig. 3), implying that paleoenvironmental conditions for sedimentary As deposition during these time intervals were not significantly different compared to the interval 6.5–2.8 ka (see discussion below).

Consistent with the surface sediment data, As/Al and IP_{25} co-vary in the 6500-year record (core JM10), with highest values between 2.8 and 6.5 ka, a decreasing trend towards 0.5 ka, and an increase towards the core-top (Fig. 4). The occurrence of IP_{25} at the core-top is consistent with modern observations of annual sea-ice formation in the polynya [19], while its presence throughout the record demonstrates persistent (but variable) seasonal sea-ice occurrence. Highest IP_{25} concentrations and As/Al ratios between 6.5 and 2.8 ka are accompanied by enhanced brassicasterol concentrations and lower relative abundances of agglutinated foraminifera (Fig. 4), implying a variable sea-ice margin and recurrent melting/freezing periods with associated phytoplankton blooms. These modern-like conditions, with seasonal sea-ice formation and increased polynyal activity, are in accordance with environmental inferences from calcareous and agglutinated foraminiferal assemblages in the fjord during this time interval [35]. Our proxy data are also consistent with simulations of increased sea-ice production (+15%) and extent (+14%) in the circum-Arctic [9], likely as a consequence of the flooding of the Arctic Siberian shelf [4] and potentially positive ocean-sea ice-atmosphere feedbacks in the Barents Sea [42], and further evidenced by

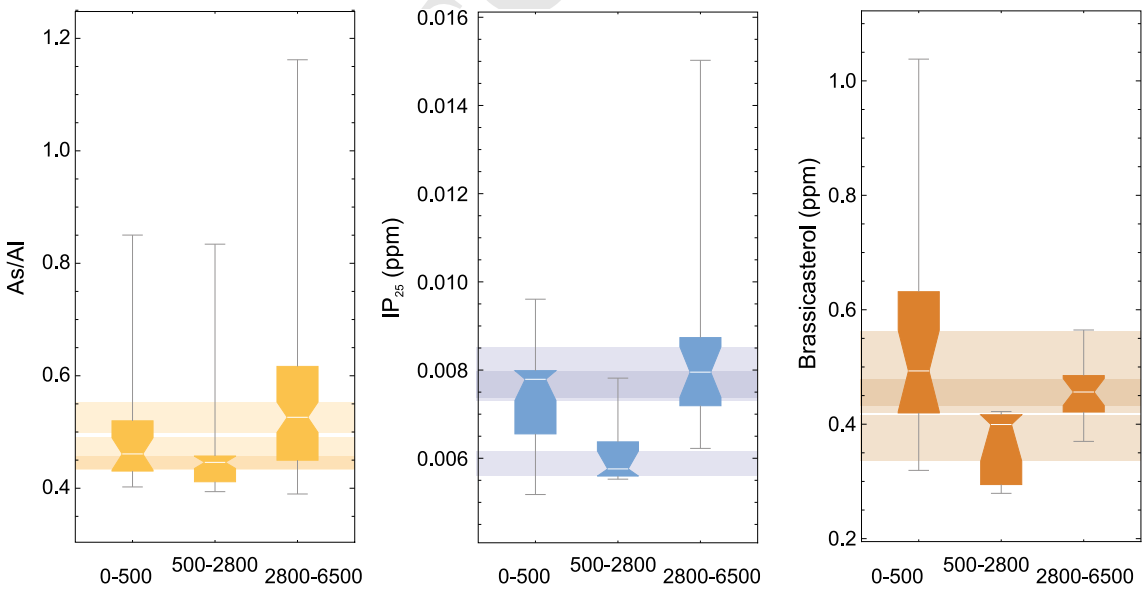

Fig. 3 Notched box-whisker plots for all down-core measurements of JM10-10GC for the parameters As/Al, IP_{25}, and brassicasterol in the time intervals 0–500 a BP, 500–2800 a BP, and 2800–6500 a BP. White lines mark the estimated positions, and notched intervals the 95%-confidence limits for the medians of the distributions

Journal : Large 41063 Dispatch : 16-12-2016 Pages : 15
Article No. : 27 LE TYPESET
MS Code : ARCT-D-16-00010 CP DISK

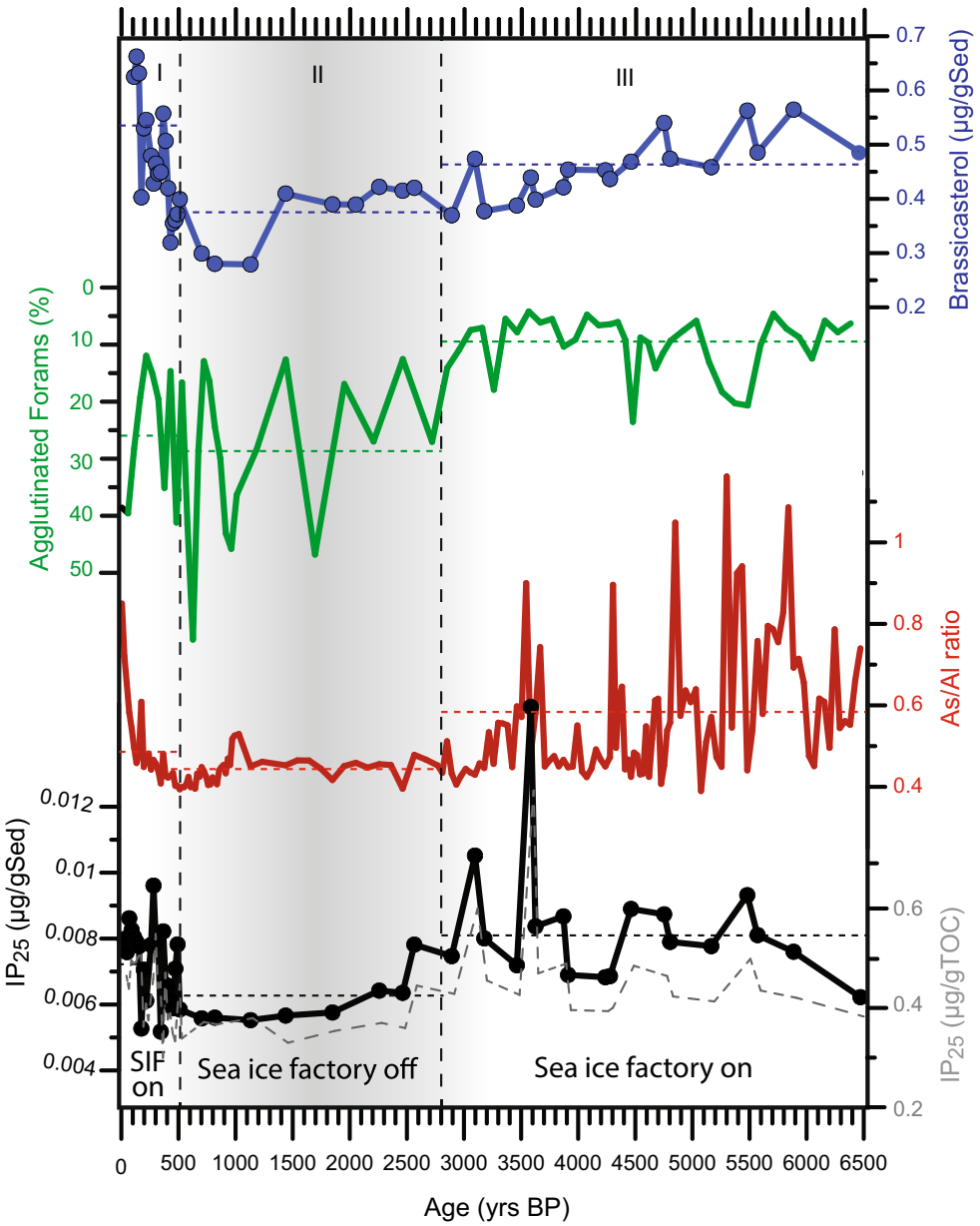

Fig. 4 Proxy data for sea-ice variability in Storfjorden polynya (core JM10-10GC) over the past 6500 years BP. Bottom to top: IP_{25} concentration (µg/gSed and µg/gTOC), As/Al ratio (×1000), agglutinated foraminifera (% of total benthic assemblages), and brassicasterol concentration (µg/gSed). *Stippled lines* indicate the mean values for each proxy in the three intervals discussed in the main text. Note that IP_{25} concentrations normalized to µg/g Sediment and µg/g TOC indicate no dilution effect on biomarker records due to variable sedimentation rates

reduced sea surface temperatures off western Svalbard around 5 ka [54] (Fig. 5). Elsewhere, a gradual southward expansion of the MIZ has been reconstructed for the Canadian Archipelago [50] and the Fram Strait [29]. Werner et al. [54] hypothesized that the occurrence of heavy winter sea-ice off the western Svalbard coast after 5.2 ka BP is due to established modern sea-ice production in the Arctic Ocean after the Holocene transgression. The distinct cooling trend in the Nordic Sea connected to the sea-ice expansion as a consequence of the flooding [9] and declining insolation [25] (Fig. 5) provides the prerequisite for the advection and persistent presence of seasonal sea-ice in the Storfjorden polynya.

A distinct change in sea-ice coverage in the Storfjorden polynya occurred after 2.8 ka BP. While a seasonally fluctuating MIZ similar to its present (winter) location prevailed along western Spitsbergen [29], the reduced sea-ice and phytoplankton biomarkers together with higher mean proportions of agglutinated foraminifera (Fig. 4) demonstrated a clear change in sea-ice conditions in the Storfjorden polynya between 2.8 and 0.5 ka, with low entrainment/freezing of terrestrial sediments, diminished surface water productivity and dense/packed sea-ice coverage. At the same time, on the western Svalbard/Barents Sea margin, decreasing values in planktic $\delta^{13}C$ records and a downward migration of the planktic foraminifera *Neogloboquadrina pachyderma* sin., also point to surface water freshening and saltier, warmer sub-surface waters (Fig. 5) [40, 55], thus preconditioning the setting for extensive sea-ice formation. The dominance of the

Journal : Large 41063 Dispatch : 16-12-2016 Pages : 15
Article No. : 27 LE TYPESET
MS Code : ARCT-D-16-00010 CP DISK

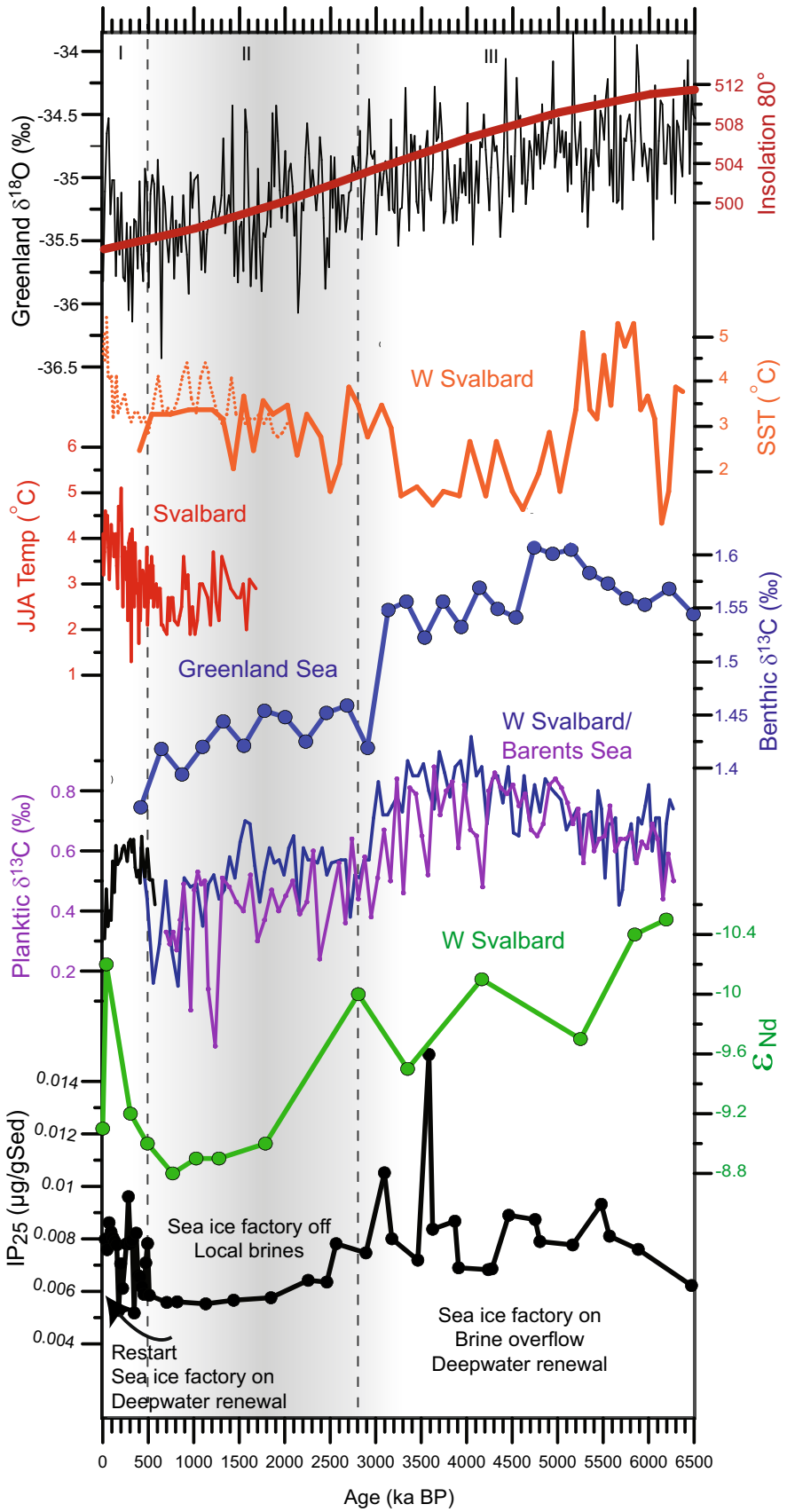

Fig. 5 Sea-ice reconstruction, brine formation and deep water penetration to the Arctic over the past 6500 years. *Bottom to* top, IP_{25} concentration (µg/gSed) in Storfjorden, seawater-derived Nd isotope variations expressed as εNd in the eastern Fram Strait [53], planktic foraminifera $\delta^{13}C$ from western Svalbard/Barents Sea [40, 54], benthic foraminiferal $\delta^{13}C$ from Greenland Sea [49], June/July/August (JJA) air temperatures over Svalbard [14], sea surface temperatures (SST) off western Svalbard [44, 54, 55], Greenland ice core data from DYE-3, GRIP and NGRIP on the GICC05 timescale [51] and solar irradiance [25]

Journal : Large 41063 Dispatch : 16-12-2016 Pages : 15
Article No. : 27 LE TYPESET
MS Code : ARCT-D-16-00010 CP DISK

calcareous benthic foraminifera species *Elphidium excavatum* in the Storfjorden sediments provides further evidence for more extensive seasonal ice cover [35]. A permanent sea-ice cover in Storfjorden is also in agreement with observations from western coastal Svalbard, where enhanced formation of shore-fast sea-ice and/or dense sea-ice coverage has been suggested [17]. On the other hand, pulses of advected Atlantic water along the Barents and Svalbard margin during this period [40, 53] did not influence the persistent sea-ice coverage in Storfjorden. However, confirmation of the latter requires a higher resolution IP_{25} record, as intervals with more variable sea-ice conditions inferred from highly fluctuating proportions of agglutinated foraminifera, which are not covered with the current IP_{25} dataset (Fig. 4). In the meantime, the high-resolution As/Al record of constantly low values (<0.5) throughout this interval implies dense sea-ice coverage, suggesting that increased proportions of agglutinated foraminifera in some intervals may reflect variable preservational conditions under the dominant influence of Arctic waters rather than strong polynyal activity, and thus brine formation. However, the latter needs to be explored further with additional records from the Storfjorden area and adjacent trough.

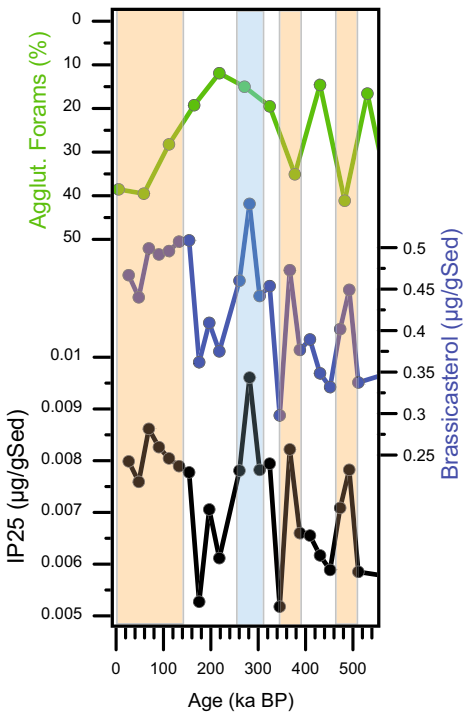

Fig. 6 Down-core variability of sea ice (IP_{25}), phytoplankton (brassicasterol), and agglutinated foraminifera indicators in Storfjorden polynya over the past ca. 500 years. *Orange bars* indicate the correspondence of high sea ice variability, phytoplankton production and strong polynyal activity as inferred from higher proportions of agglutinated foraminifera [34]. *Blue bar* shows no response

Rapidly increasing phytoplankton production, and enhanced IP_{25} concentrations demonstrate that the sea-ice factory restarted abruptly ~0.5 ka BP, at which time, sediment entrainment/release processes also recovered, with higher As/Al ratios towards the core-top (Fig. 4). The establishment of a highly fluctuating sea-ice boundary would have finally led to formation of a coastal polynya with seasonally variable sea-ice conditions. Enhanced IP_{25} and brassicasterol concentrations are largely consistent (except one interval centered on 0.3 ka) with increased proportions of agglutinated foraminifera (Fig. 6), supporting inferences by Rasmussen and Thomsen [34] of an intensified but variable polynyal activity. Thus, constantly high sea-ice production throughout the last ~500 years is likely the result of inferred mild summer temperatures on Spitsbergen including the Little Ice Age (Fig. 5) [14]. These modern-like conditions in Storfjorden, with variable sea-ice coverage over the last 500 years, contrast the more dense/packed sea-ice conditions in the preceding interval (~2.8–0.5 ka BP), but corroborate a recent biomarker-based sea-ice reconstruction for western Svalbard, which showed a gradual decline in spring sea-ice concentration over the past 400 years [12].

Relationship between sea-ice, brines and deep water production

In modern times, it is well known that dynamic sea-ice production and brine rejection within the wind-driven polynyas in the circum-Arctic are important contributors for deep water convection in the Nordic Seas and Arctic Ocean [2, 41, 43]. Further, Bauch et al. [4] suggested that for the Last Glacial Maximum, enhanced sea-ice production and dense bottom water formation could be attributed to the formation of katabatic wind-driven polynyas in front of the western Svalbard-Barents Sea ice sheet. Similarly, based on calcareous and agglutinated foraminifera, Rasmussen and Thomsen [34, 35] showed that the strength of brine formation in the Storfjorden polynya over the last 15 ka BP was largely related to climatic conditions, with enhancements during cold periods (and vice versa). However, such studies were based on rather unselective proxies for sea-ice reconstruction (i.e. stable isotopes and assemblages of benthic and planktic foraminifera), which potentially limits their value in terms of confirming the significance of brine rejection on deep water formation in palaeo records (Table 5).

In this study, we demonstrate temporal coherence between our more direct proxy-based sea-ice reconstruction (and inferred brine intensity changes) and changes to deep water convection obtained from local and other regional records from the Nordic Seas (Fig. 5). Thus, the recurrent freezing/melting of sea-ice in the Storfjorden

Journal : Large 41063 Dispatch : 16-12-2016 Pages : 15
Article No. : 27 LE TYPESET
MS Code : ARCT-D-16-00010 CP DISK

Table 5 Down-core variability of IP_{25} concentrations in JM10-10GC

Depth_cm	Age_a_BP1950	IP25com µg/gSed	IP25com µg/gTOC
2.5	26.57	0.00799	0.467
4.5	47.83	0.00759	0.440
6.5	69.09	0.00862	0.499
8.5	90.35	0.00826	0.492
10.5	111.61	0.00804	0.496
12.5	132.87	0.00789	0.507
14.5	154.12	0.00777	0.509
16.5	175.38	0.00527	0.362
18.5	196.64	0.00706	0.409
20.5	217.90	0.00612	0.375
24.5	260.42	0.00781	0.460
26.5	281.67	0.00961	0.553
28.5	302.93	0.00782	0.442
30.5	324.19	0.00794	0.454
32.5	345.45	0.00518	0.298
34.5	366.71	0.00822	0.473
36.5	387.97	0.00660	0.377
38.5	409.22	0.00655	0.389
40.5	430.48	0.00617	0.349
42.5	451.74	0.00589	0.332
44.5	473.00	0.00709	0.402
46.5	492.17	0.00782	0.449
48.5	511.34	0.00585	0.337
68.5	703.07	0.00558	0.371
80.5	818.10	0.00560	0.367
104.5	1131.41	0.00553	0.379
110.5	1438.65	0.00566	0.329
118.5	1848.29	0.00576	0.353
126.5	2257.94	0.00642	0.370
130.5	2462.76	0.00636	0.359
132.5	2565.18	0.00782	0.446
142.5	2892.27	0.00747	0.429
152.5	3096.05	0.01052	0.605
156.5	3177.57	0.00801	0.457
170.5	3462.86	0.00719	0.427
176.5	3585.14	0.01502	0.849
178.5	3625.89	0.00837	0.472
190.5	3870.43	0.00867	0.492
192.5	3911.19	0.00690	0.396
208.5	4237.24	0.00683	0.394
210.5	4278.00	0.00686	0.401
224.5	4462.45	0.00890	0.487
246.5	4752.30	0.00874	0.466
250.5	4805.00	0.00790	0.424
266.5	5165.16	0.00777	0.414
280.5	5480.30	0.00932	0.502
284.5	5570.34	0.00811	0.436
298.5	5885.48	0.00760	0.421
324.5	6470.74	0.00622	0.383

Journal : Large 41063 Dispatch : 16-12-2016 Pages : 15
Article No. : 27 ☐ LE ☐ TYPESET
MS Code : ARCT-D-16-00010 ☑ CP ☑ DISK

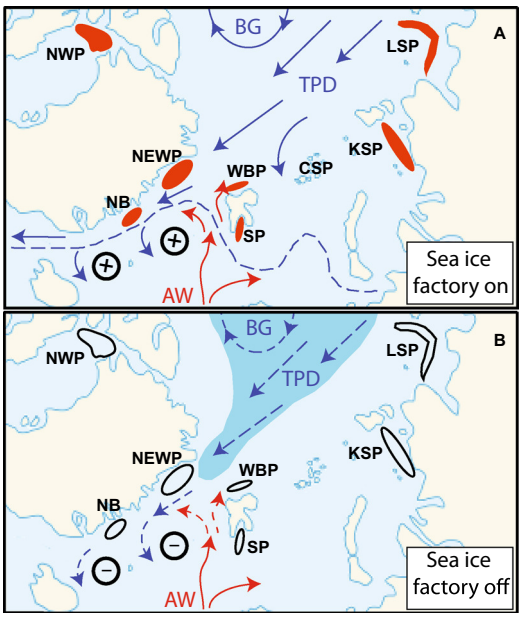

Fig. 7 Location of coastal polynyas in the Arctic with variable sea-ice dynamics. **a** Modern sea-ice distribution and strong deep convections (*crosses*) with vigorous sea-ice factories (*orange polygons*) for brine-enriched shelf water formation. *Blue arrows* cold, ice-covered surface currents. Red arrows: warm, saline Atlantic-derived water masses. **b** Less sea-ice in the Arctic with shut down of sea-ice factories (*open polygons*) and slow down of deep convection (minus). *NWP* North Water polynya, *NEWP* Northeast Water polynya, *NB* Nordbukta, *WBP* Whaler's Bay polynya, *SP* Storfjorden Polynya, *KSP* Kara Sea polynya, *LSP* Laptev Sea polynya

polynya and associated strong brine formation between 6.5 and 2.8 ka BP coincides with less radiogenic ε_{Nd} values (−9.4 to −10.6) from western Spitsbergen, as seen for present-day deep water penetration to the Arctic Ocean [53] (Fig. 5). During the same interval, high convection rates in most areas of the Nordic Seas is evident from high carbon isotope values in both planktic and benthic foraminifera [4, 40], together with a period of maximum ventilation in the Greenland Sea (Fig. 5) [48, 49] and AMOC strengthening [20]. In contrast, more permanent sea-ice cover and probably subdued brine formation in Storfjorden polynya after 2.8 ka, is accompanied by a prominent shift to more radiogenic ε_{Nd} along the western Spitsbergen continental margin (Fig. 5) [53]. At the same time, freshening of surface waters and intensification (thickening) of sea-ice in the Fram Strait has been deduced from carbon isotope data of planktic foraminifera [54] (Fig. 5) and elevated IP_{25} abundances [29], while increased sea-ice production in the Arctic and export through Fram Strait also coincides with a proposed reduction of deep convection in the Greenland Sea [49] (Fig. 5). Modelling results also suggest that negative anomalies in total solar irradiance ~2.7 ka may have been responsible for local shutdown of deep water formation in the Nordic Seas at this time [39], which when superimposed on decreasing insolation (Fig. 5) may have stimulated positive oceanic feedbacks, such as enhanced stratification, expansion of sea-ice and less deep water formation leading to additional cooling and more sea-ice (e.g. [48, 49]. Regardless of the ultimate trigger for the abrupt changes in sea-ice coverage in Storfjorden polynya at ~2.8 ka, the timing of such solar-forced cooling events demonstrates that the most severe climatic conditions in the Nordic Seas and circum-Arctic reduced the contribution of Arctic sea-ice factories (i.e. polynyas) to deep water production.

The enhancement of the sea-ice factory and phytoplankton production in Storfjorden at ~0.5 ka BP, when recurrent freezing/melting of sea-ice in the polynya coincides largely with the increased admixture of deep waters from the Nordic Sea (less radiogenic ε_{Nd}) (Fig. 5) and increased proportions of agglutinated foraminifera (Fig. 6), supports the notion of enhanced brine formation during stronger polynyal activity. The transition to more intense polynyal activity ~0.5 ka BP, coupled to higher sea-ice variability thereafter, also aligns with observations from western Svalbard, where spring sea-ice concentration has steadily declined over the past 400 years [12] and heat transport into the Arctic via the West Spitsbergen Current has increased [14, 44].

Implications and conclusions

The Arctic Ocean halocline is maintained by the contribution of cold and brine-enriched deep waters [1, 13], which are formed because of high sea-ice production in coastal polynyas over the continental shelves (Fig. 7) [47]. Tamura and Ohshima [47] showed that the current polar amplification of global warming will lead to negative trends in sea-ice production in most of the Arctic polynyas and with future projections of a summer ice-free Arctic Ocean (IPCC 2013), sea-ice factories in Arctic coastal polynyas may lose their significance entirely (Fig. 7). A likely cause for this trend could be delayed sea-ice freezing and increased Arctic air temperatures [47]. The last time a similar scenario occurred was during the Holocene Thermal Maximum when Arctic Ocean sea-ice cover was believed to be less than half of the minimum summer extent in 2007 [18]. Indeed, Årthun et al. [58] showed that during periods of maximum warming in the central Barents Sea, formation of brine-enriched shelf waters, and thus export of deep waters to the Nordic Seas and Arctic Ocean, was strongly reduced. Whether this reduced export contributed to the slow down in AMOC in the twentieth century (Rahmstorf et al. 2015) remains speculative. However, AQ9 from this study we conclude that sea-ice production in Arctic coastal polynyas is highly sensitive to variable, externally forced climate or ocean feedback mechanisms.

Journal : Large 41063 Dispatch : 16-12-2016 Pages : 15
Article No. : 27 ☐ LE ☐ TYPESET
MS Code : ARCT-D-16-00010 ☑ CP ☑ DISK

The correspondence between high (low) polynyal activity and variable sea-ice conditions in one important Arctic sea-ice factory, and observations of stronger (weaker) deep water renewal processes in the Nordic Seas during the present interglacial highlight the potential consequences for ocean ventilation during states with permanent sea-ice cover or future Arctic ice-free conditions.

Acknowledgements This work is a contribution to the CASE Initial Training Network funded by the European Community's 7th Framework Programme FP7 2007/2013, Marie-Curie Actions, under Grant Agreement No. 238111. The research is part of the Centre for Arctic Gas Hydrate, Environment and Climate and was supported by the Research Council of Norway through its Centres of Excellence funding scheme Grant No. 223259.

References

1. Aagaard K, Coachman L, Carmack E (1981) On the halocline of the Arctic Ocean. Deep Sea Res Part a Oceanogr Res Pap 28:529–545. doi:10.1016/0198-0149(81)90115-1
2. Aagaard K, Swift J, Carmack E (1985) Thermohaline circulation in the Arctic Mediterranean Seas. J Geophys Res 90:4833–4846
3. Alonso-Garcia M, Andrews JT, Belt S, Cabedo-Sanz P, Darby D, Jaeger J (2013) A comparison between multi-proxy and historical data (AD 1990—1840) of drift-ice conditions on the East Greenland shelf (~66°N). The Holocene 23:1872–1883
4. Bauch HA et al (2001) Chronology of the Holocene transgression at the North Siberian margin. Glob Planet Change 31:125–139
5. Belt S, Brown TA, Navarro-Rodriguez A, Cabedo-Sanz P, Tonkin A, Ingle R (2012) A reproducible method for the extraction, identification and quantification of the Arctic sea ice proxy IP25 from marine sediments. Anal Methods 4:705–713
6. Belt S, Müller J (2013) The Arctic sea ice biomarker IP25: a review of current understanding, recommendations for future research and applications in palaeo sea ice reconstructions. Quat Sci Rev 79:9–25. doi:10.1016/j.quascirev.2012.12.001
7. Belt ST, Cabedo-Sanz P, Smik L, Navarro-Rodriguez A, Berben SMP, Knies J, Husum K (2015) Identification of paleo Arctic winter sea ice limits and the marginal ice zone: optimised biomarker-based reconstructions of late Quaternary Arctic sea ice. Earth Planet Sci Lett 431:127–139. doi:10.1016/j.epsl.2015.09.020
8. Belt ST, Massé G, Rowland SJ, Poulin M, Michel C, LeBlanc B (2007) A novel chemical fossil of palaeo sea ice: IP25. Org Geochem 38:16–27. doi:10.1016/j.orggeochem.2006.09.013
9. Blaschek M, Renssen H (2013) The impact of early Holocene Arctic shelf flooding on climate in an atmosphere-ocean-sea-ice model. Clim Past 9:2651–2667. doi:10.5194/cp-9-2651-2013
10. Broecker WS, Peng T-H (1982) Tracers in the sea. Lamont-Doherty Geological Observatory Columbia University, New York
11. Brown TA, Belt ST, Tatarek A, Mundy CJ (2014) Source identification of the Arctic sea ice proxy IP25. Nat Commun. doi:10.1038/ncomms5197
12. Cabedo-Sanz P, Belt S (2016) Seasonal sea ice variability in eastern Fram Strait over the last 2000 years. Arktos 2:22. doi:10.1007/s41063-41016-40023-41062
13. Cavalieri DJ, Martin S (1994) The contribution of Alaskan, Siberian, and Canadian coastal polynyas to the cold halocline layer of the Arctic Ocean. J Geophys Res Oceans 99:18343–18362. doi:10.1029/94jc01169
14. D'Andrea WJ, Vaillencourt DA, Balascio NL, Werner A, Roof SR, Retelle M, Bradley RS (2012) Mild Little Ice Age and unprecedented recent warmth in an 1800 year lake sediment record from Svalbard. Geology 40:1007–1010. doi:10.1130/g33365.1
15. Dokken TM, Jansen E (1999) Rapid changes in the mechanism of ocean convection during the last glacial period. Nature 401:458–461. doi:10.1038/46753
16. Eicken H, Reimnitz E, Alexandrov V, Martin T, Kassens H, Viehoff T (1997) Sea-ice processes in the Laptev Sea and their importance for sediment export. Cont Shelf Res 2:205–233
17. Forwick M, Vorren T (2009) Late Weichselian and Holocene sedimentary environments and ice rafting in Isfjorden, Spitsbergen. Palaeogeogr Palaeoclimatol Palaeoecol. doi:10.1016/j.palaeo.2009.06.026
18. Funder S et al. (2011) A 10,000-year record of arctic ocean sea-ice variability-view from the beach. Science 333:747–750. doi:10.1126/science.1202760
19. Haarpaintner J, Gascard J-C, Haugan PM (2001) Ice production and brine formation in Storfjorden, Svalbard. J Geophys Res 106:14001–14013
20. Hall I, Bianchi G, Evans J (2004) Centennial to millennial scale Holocene climate–deep water linkage in the North Atlantic. Quat Sci Rev 23:1529–1536
21. Hölemann JA, Schirmacher M, Kassens H, Prange A (1999) Geochemistry of surficial and ice-rafted sediments from the Laptev Sea (Siberia) Estuarine. Coast Shelf Sci 49:45–59. doi:10.1006/ecss.1999.0485
22. Jensen H (2000) Resultater av kjemiske analyser av prøver av Svalbard kull og tilgrensende bergarter over, under og mellom kull fløtsene. NGU, Trondheim
23. Jungclaus JH, Backhaus JO, Fohrmann H (1995) Outflow of dense water from the Storfjord in Svalbard: a numerical model study. J Geophys Res Oceans 100:24719–24728. doi:10.1029/95jc02357
24. Killworth PD (1983) Deep convection in the World Ocean. Rev Geophys 21:1–26. doi:10.1029/RG021i001p00001
25. Laskar J, Robutel P, Joutel F, Gastineau M, Correia ACM, Levrard B (2004) A long-term numerical solution for the insolation quantities of the Earth. Astron Astrophys 428:261–285. doi:10.1051/0004-6361:20041335
26. Loring DH, Dahle S, Naes K, Dos Santos J, Skei JM, Matishov GG (1998) Arsenic and other trace metals in sediments from the Kara Sea and the Ob and Yenisey Estuaries. Russia Aquat Geochem 4:233–252. doi:10.1023/A:1009691314353
27. Loring DH, Næs K, Dahle S, Matishov GG, Illin G (1995) Arsenic, trace metals, and organic micro contaminants in sediments from the Pechora Sea, Russia. Mar Geol 128:153–167. doi:10.1016/0025-3227(95)00091-C
28. Mackensen A, Schmiedl G (2016) Brine formation recorded by stable isotopes of Recent benthic foraminifera in Storfjorden: palaeoceanographical implications. Boreas 45:552–566. doi:10.1111/bor.12174
29. Müller J, Werner K, Stein R, Fahl K, Moros M, Jansen E (2012) Holocene cooling culminates in sea ice oscillations in Fram Strait. Quat Sci Rev 47:1–14. doi:10.1016/j.quascirev.2012.04.024
30. Navarro-Rodriguez A, Belt ST, Knies J, Brown TA (2013) Mapping recent sea ice conditions in the Barents Sea using the proxy biomarker IP25: implications for palaeo sea ice reconstructions. Quat Sci Rev. doi:10.1016/j.quascirev.2012.11.025
31. Ottesen RT et al (2010) Geochemical atlas of Norway, Part 2: Geochemical atlas of Spitsbergen. Chemical composition of overbank sediments. Norges geologiske undersøkelse/Norges vassdrags- og energidirektorat, Trondheim

Journal : Large 41063 Dispatch : 16-12-2016 Pages : 15
Article No. : 27 ☐ LE ☐ TYPESET
MS Code : ARCT-D-16-00010 ✔ CP ✔ DISK

32. Quadfasel D, Rudels B, Kurz K (1988) Outflow of dense water from a Svalbard fjord into the Fram Strait. Deep Sea Res Part A Oceanogr Res Pap 35:1143–1150. doi:10.1016/0198-0149(88)90006-4
33. Rasmussen TL, Thomsen E (2009) Stable isotope signals from brines in the Barents Sea: implications for brine formation during the last glaciation. Geology 37:903–906. doi:10.1130/g25543a.1
34. Rasmussen TL, Thomsen E (2014) Brine formation in relation to climate changes and ice retreat during the last 15,000 years in Storfjorden, Svalbard, 76–78°N. Paleoceanography 29:911–929. doi:10.1002/2014pa002643
35. Rasmussen TL, Thomsen E (2015) Palaeoceanographic development in Storfjorden, Svalbard, during the deglaciation and Holocene: evidence from benthic foraminiferal records. Boreas 44:24–44. doi:10.1111/bor.12098
36. Reigstad M, Carroll J, Slagstad D, Ellingsen I, Wassmann P (2011) Intra-regional comparison of productivity, carbon flux and ecosystem composition within the northern Barents Sea. Prog Oceanogr 90:33–46. doi:10.1016/j.pocean.2011.02.005
37. Reimann C, Matschullat J, Birke M, Salminen R (2009) Arsenic distribution in the environment: the effects of scale. Appl Geochem 24:1147–1167. doi:10.1016/j.apgeochem.2009.03.013
38. Reimer PJ et al (2013) IntCal13 and Marine13 radiocarbon age calibration curves, 0–50,000 years cal BP. Radiocarbon 55:1869–1887
39. Renssen H, Goosse H, Muscheler R (2006) Coupled climate model simulation of Holocene cooling events: oceanic feedback amplifies solar forcing. Clim Past 2:79–90
40. Sarnthein M, Van Kreveld S, Erlenkeuser H, Grootes PM, Kucera M, Pflaumann U, Schulz M (2003) Centennial-to-millennial-scale periodicities of Holocene climate and sediment injections off the western Barents shelf, 75 degrees N. Boreas 32:447–461. doi:10.1080/03009480310003351
41. Schauer U (1995) The release of brine-enriched shelf water from Storfjord into the Norwegian Sea. J Geophys Res Oceans 100:16015–16028. doi:10.1029/95jc01184
42. Semenov VA, Park W, Latif M (2009) Barents Sea inflow shutdown: a new mechanism for rapid climate changes. Geophys Res Lett. doi:1029/2009gl038911
43. Skogseth R, Haugan PM, Haarpaintner J (2004) Ice and brine production in Storfjorden from four winters of satellite and in situ observations and modeling. J Geophys Res Oceans. doi:10.1029/2004jc002384
44. Spielhagen RF et al (2011) Enhanced modern heat transfer to the Arctic by warm Atlantic water. Science 331:450–453. doi:10.1126/science.1197397
45. Stuiver M, Reimer PJ (1993) Extended C-14 data-base and revised CALIB 3.0 C-14 AGE calibration program. Radiocarbon 35:215–230
46. Sullivan KA, Aller RC (1996) Diagenetic cycling of arsenic in Amazon shelf sediments. Geochim Cosmochim Acta 60:1465–1477. doi:10.1016/0016-7037(96)00040-3
47. Tamura T, Ohshima KI (2011) Mapping of sea ice production in the Arctic coastal polynyas. J Geophys Res. doi:10.1029/2010jc006586
48. Telesiński MM, Bauch HA, Spielhagen RF, Kandiano ES (2015) Evolution of the central Nordic Seas over the last 20 thousand years. Quat Sci Rev 121:98–109
49. Telesiński MM, Spielhagen RF, Bauch HA (2014) Water mass evolution of the Greenland Sea since late glacial times. Clim Past 10:123–136. doi:10.5194/cp-10-123-2014
50. Vare L, Massé G, Gregory T, Smart C, Belt S (2009) Sea ice variations in the central Canadian Arctic Archipelago during the Holocene. Quat Sci Rev 28:1354–1366. doi:10.1016/j.quascirev.2009.01.013
51. Vinther BM et al (2006) A synchronized dating of three Greenland ice cores throughout the Holocene. J Geophys Res. doi:10.1029/2005jd006921
52. Wedepohl KJ (1991) The composition of the upper earth's crust and the natural cycles of selected metals. Metals in natural raw materials. Natural resources. In: Merian E (ed) Metals and their compounds in the environment. VCH, Weinheim, pp 3–17
53. Werner K, Frank M, Teschner C, Mueller J, Spielhagen RF (2014) Neoglacial change in deep water exchange and increase of sea-ice transport through eastern Fram Strait: evidence from radiogenic isotopes. Quat Sci Rev 92:190–207. doi:10.1016/j.quascirev.2013.06.015
54. Werner K, Spielhagen RF, Bauch D, Hass HC, Kandiano E (2013) Atlantic water advection versus sea-ice advances in the eastern Fram Strait during the last 9 ka: multiproxy evidence for a two-phase Holocene. Paleoceanography 28:283–295. doi:10.1002/palo.20028
55. Werner K, Spielhagen RF, Bauch D, Hass HC, Kandiano E, Zamelczyk K (2011) Atlantic Water advection to the eastern Fram Strait—multiproxy evidence for late Holocene variability. Palaeogeogr Palaeoclimatol Palaeoecol 308:264–276. doi:10.1016/j.palaeo.2011.05.030
56. Winkelmann D, Knies J (2005) Recent distribution and accumulation of organic carbon on the continental margin west off Spitsbergen. Geochem Geophys Geosyst. doi:10.1029/2005gc000916
57. Xiao X, Fahl K, Müller J, Stein R (2015) Sea-ice distribution in the modern Arctic Ocean: biomarker records from trans-Arctic Ocean surface sediments. Geochim Cosmochim Acta 155:16–29
58. Årthun M, Ingvaldsen RB, Smedsrud LH, Schrum C (2011) Dense water formation and circulation in the Barents Sea. Deep Sea Res Part I 58:801–817. doi:10.1016/j.dsr.2011.06.001

Journal : Large 41063 Dispatch : 16-12-2016 Pages : 15
Article No. : 27 ☐ LE ☐ TYPESET
MS Code : ARCT-D-16-00010 ☑ CP ☑ DISK